Buckling under the action of loading by aerodynamic and inertial forces during ground track tests of aviation equipment

Sergey A. ASTAKHOV*,[1], Vasiliy I. BIRYUKOV[2]

*Corresponding author
[1]State Governmental Scientific-Testing Area of Aircraft Systems,
Beloozersky, 140250, Russian Federation,
info@gknipas.ru*
[2]Department No. 904, Moscow Aviation Institute (National Research University),
4 Volokolamskoe Shosse, 125993, Moscow, Russian Federation,
aviatex@mail.ru

DOI: 10.13111/2066-8201.2021.13.S.1

Received: 10 March 2021/ Accepted: 28 June 2021/ Published: August 2021

Abstract: *The article analyses the choice of a rational layout of the test object with a propulsion system (PS). One of the design examples of calculating the longitudinal stability and strength of the structure is given. The purpose of the article is to solve the problem of bending the elastic line of a cantilever tubular rod with a hinged termination during tests of a propulsion system for various aircrafts. On the example, the estimates of the approximate test object, accelerated on the track to a speed of 1200 m/s, are carried out. The aerodynamic loading of the structure of the mobile track installation is considered using the methods of mathematical modelling and the development of an algorithm for the numerical solution of the problem of bending the elastic line of a cantilever tubular rod. The deflection from the forces of external and internal loads of the outer shell of a movable track installation is considered, provided that the diameter of the outer contour is equal to the minimum and it is constant along the entire length.*

Key Words: *movable installation, construction, resistance forces*

1. INTRODUCTION

The problems that arise before the designers of various types of aircraft require their consistent solution through ground track full-scale tests. To ensure reliability during high-speed testing of aircraft products, preliminary design estimates of the strength and stability of structural units are required, taking into account the influence of various factors when the maximum speed of the test object is reached. The practical implementation of ground track tests of aircraft objects is preceded by mathematical modelling and the development of an algorithm for the numerical solution of a problem that simulates test conditions [1], [2], [3]. The problems that arise before the designers of various types of aircraft require their consistent solution through ground track full-scale tests. To ensure reliability during high-speed testing of aircraft products, preliminary design estimates of the strength and stability of structural units are required, taking into account the influence of various factors when the maximum speed of the test object is reached. The practical implementation of ground track tests of

aircraft objects is preceded by mathematical modelling and the development of an algorithm for the numerical solution of a problem that simulates test conditions [4], [5]. Ground high-speed tests of various objects of aviation technology are carried out on an experimental track installation 3,500 m long. The track itself is a two-rail track that guides the movement of the test object placed on a track carriage, on two rails, or on a monorail [6], [7], [8], [9], [10].

The acceleration of the rail carriage is provided by a solid propellant rocket engine (SPRE). The test object is a hollow cylinder with a tapered fairing. The track carriage with welded-on shoes (conventionally sleeve bearings) can move freely along the rail. The shoes play the role of a hinged termination.

2. MATERIALS AND METHODS

Let us consider the aerodynamic loading of the structure of a mobile track installation. On the one hand, the thrust force of the SPRE is directed along the axis of the installation in the direction of travel; we denote it as R. On the other hand, the forces of aerodynamic resistance are directed against the direction of motion; we denote them as P_{Σ}. In this case, it is the total value of various types of aerodynamic drag, including wave drag. The forces of resistance to sliding friction caused by the normal force of pressure on the bearing surface of the shoes are also taken into account [6], [7], [11], [12], [13], as well as the loss of the traction force due to the creation of the lifting force due to the positive angle of inclination of the rail (angle of attack) when the carriage moves along the rail track [6], [14], [15]. The magnitude of the lifting force is variable during the movement of the rail carriage. The installation diagram is presented in Figure 1.

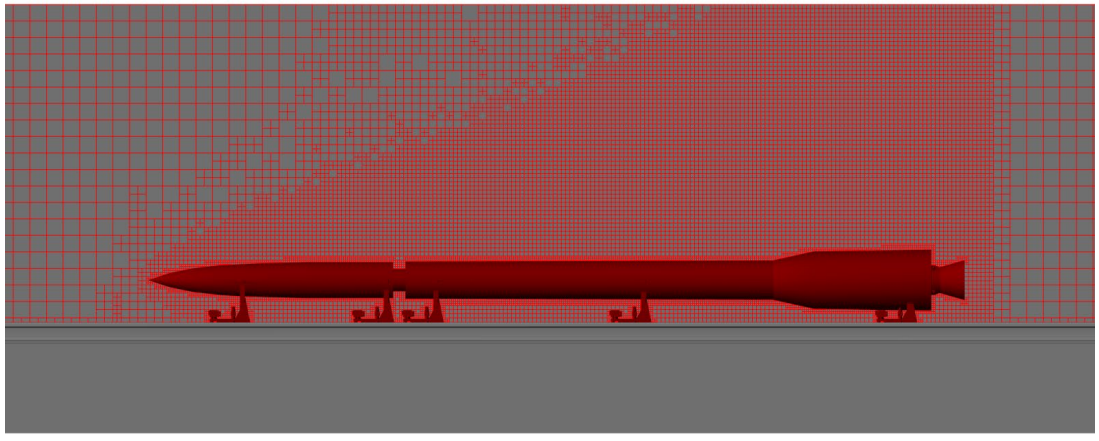

Fig. 1 – Image of the test object, placed on a track carriage with solid propellant motors

We consider a cantilever-mounted nose (a cylinder with a docked conical fairing without supports, in contrast to Fig. 1) and PS on two supports (shoes). One support is displaced 0.5 m from the joint with the nose, and the other retreats 0.5 m from the tail of the engine.

3. RESULTS AND DISCUSSIONS

Let us consider the deflection from the forces of external and internal loads of the outer shell of a movable track installation, provided that the diameter of the outer contour is equal to the minimum and is constant along the entire length. Equation of balance of forces:

$$P_{\Sigma aer}(t) + R(t) = P_{\Sigma}(t), \tag{1}$$

where: $R(t)$ is the thrust force of the SPRE; $P_{\Sigma aer}(t)$ is total aerodynamic drag forces; $P_{\Sigma}(t)$ is the total compression force of the shell (tubular rod).

We denote the longitudinal axis of the mobile installation by x; it is directed parallel to the rail track along the movement.

The y-axis is perpendicular to the motion and is the direction of deflection of the elastic line of the tubular rod [16], [17], [18]. At small deformations within Hooke's law, the deflection equation will have the form [11]:

$$EJ\frac{d^2y}{dx^2} = \pm M_{\text{BEND}}(x), \tag{2}$$

here: E – modulus of elasticity; J – the smallest moment of inertia of the section of the cylindrical part of the console. The bending moment in the current section x will be equal to:

$$M_{\text{BEND}}(x) = P_{\text{LAT}} \cdot x - P_{\Sigma}(t) \cdot y, \tag{3}$$

P_{LAT} is lateral force arising from the interaction of shock waves around the bow and reflected from the track surface when tested on a monorail (Fig. 2).

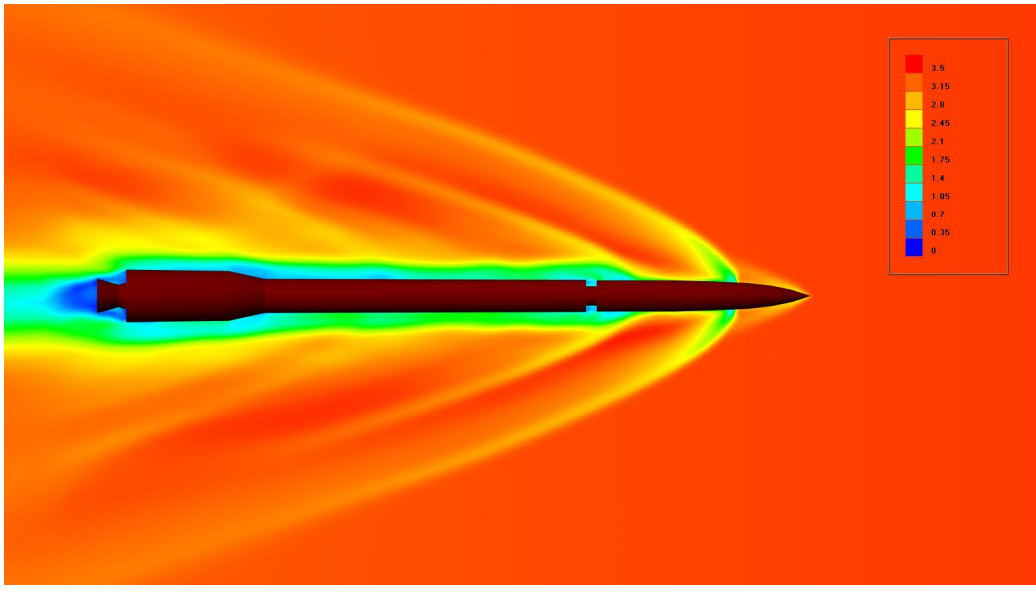

Fig. 2 – Image of the shock wave interference when the rail carriage moves at a speed of 1200 m/s. (The calculation was performed in Flow Vision)

Elastic line differential equation:

$$EJ\frac{d^2y}{dx^2} = P_{\text{LAT}} \cdot x - P_{\Sigma}(t) \cdot y, \tag{4}$$

The differential equation of the elastic line of the structure:

$$\frac{d^2y}{dx^2} + \frac{P_{\Sigma}(t)}{EJ} \cdot y = \frac{P_{\text{LAT}}}{EJ} \cdot x. \tag{5}$$

The general solution to this differential equation is:

$$y = A\,sin\sqrt{\frac{P_\Sigma(t)}{EJ}}x + B\,cos\sqrt{\frac{P_\Sigma(t)}{EJ}}x + \frac{P_{\text{LAT}}(t)}{P_\Sigma(t)}x, \tag{6}$$

for simplicity, we introduce the notation: the angle α is represented as follows:

$$\alpha = \sqrt{\frac{P_\Sigma(t)}{EJ}}, \tag{7}$$

and the equation of the elastic line is written in the form:

$$y = A\,sin\,\alpha\,x + B\,cos\,\alpha\,x + \frac{P_{\text{LAT}}}{P_\Sigma}\cdot x. \tag{8}$$

For an arbitrary moment in time, let us estimate the values of the constants [19]. Provided that the shoe touches the bottom surface of the rail head for the moment of time of reaching the maximum speed and on the ascending section of the track with an inclination angle equal to α = 1.15° (tan α = 0.02), we assume that at $x = 0$ the transverse deflection is zero, i.e., $y = 0$; from here follows $B = 0$. For the case under consideration, shoes No. 1, No. 2, No. 4 (see Fig. 1) do not exist. We consider shoe No. 3 to be a hinged termination. Bending of the bar is realised along the curve of least resistance (least stiffness). Interest in the problem under consideration was manifested in works [20], [21], [22], [23], [24], [25], [26].

Next, we consider the problem of bending the elastic line of a cantilever tubular rod bounded by support No. 3, which we now consider to be a hinged termination. The elastic line equation [27] is described by the equation:

$$y = A\,sin\,\alpha\,x + \frac{P_{\text{LAT}}}{P_\Sigma}\cdot x. \tag{9}$$

An approximate deflection can be represented by the dependence (Fig. 3):

$$y(x) = a_0 + a_1x + a_2x^2 + a_3x^3 + \ldots + a_nx^n, \tag{10}$$

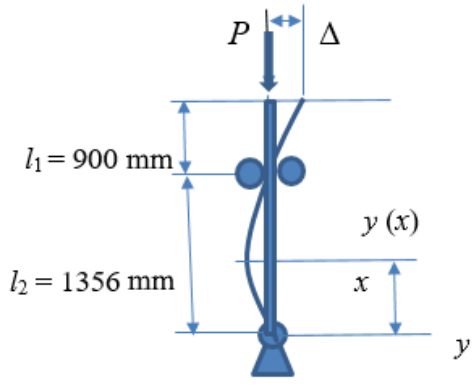

Fig. 3 – Simplified diagram of the deflection of an elastic line.

To determine the coefficients, we formulate the boundary conditions for the considered scheme: $y(0) = 0$; $y''(0) = 0$; $y(l_2) = 0$; $y''(l_1 + l_2) = 0$; $y(l_1 + l_2) = \Delta$ is the required deflection of the fairing apex from the axis. From the first two conditions it follows that $a_0 = 0$, $a_2 = 0$. From the third and fourth conditions we obtain:

$$y(l_2) = a_1 l_2 + a_3 {l_2}^3 + a_4 {l_2}^4 = 0, \tag{11}$$

$$y''(x) = a_3 + 2a_4(l_1 + l_2) = 0. \tag{12}$$

Let us express the coefficients:

$$a_3 = -2a_4(l_1 + l_2), \tag{13}$$

$$a_1 l_2 + (-2a_4(l_1 + l_2)){l_2}^3 + a_4 {l_2}^4 = 0, \tag{14}$$

$$a_1 = a_4\left[2(l_1 + l_2){l_2}^2 - {l_2}^3\right] = a_4\left(2l_1 \cdot {l_2}^2 + {l_2}^3\right) \tag{15}$$

The equation of the elastic line of the mobile unit will take the form:

$$y(x) = a_4\left(2l_1 \cdot {l_2}^2 + {l_2}^3\right)x - 2a_4(l_1 + l_2)x^3 + a_4 x^4, \tag{16}$$

$$y'(x) = a_4\left(2l_1 \cdot {l_2}^2 + {l_2}^3\right) - 6a_4(l_1 + l_2)x^2 + 4a_4 x^3, \tag{17}$$

$$y''(x) = 12a_4 x^2 - 12a_4(l_1 + l_2)x = 12a_4[x^2 - (l_1 + l_2)x], \tag{18}$$

$$\begin{gathered}[y'(x)]^2 = a_4^2\left(2l_1 \cdot {l_2}^2 + {l_2}^3\right)^2 + 36a_4^2(l_1 + l_2)^2 x^4 + 16a_4^2 x^6 - \\ - 12a_4^2\left(2l_1 \cdot {l_2}^2 + {l_2}^3\right)(l_1 + l_2) + 8a_4^2\left(2l_1 \cdot {l_2}^2 + {l_2}^3\right)x^3 - 48a_4^2(l_1 + l_2)x^3,\end{gathered} \tag{19}$$

$$\begin{gathered}[y'(x) = 16a_4^2 x^6 - 48a_4^2(l_1 + l_2)x^5 + 36a_4^2(l_1 + l_2)^2 x^4 + 8a_4^2\left(2l_1 \cdot {l_2}^2 + {l_2}^3\right)x^3 \\ -12a_4^2\left(2l_1 \cdot {l_2}^2 + {l_2}^3\right)(l_1 + l_2)x^2 + a_4^2\left(2l_1 \cdot {l_2}^2 + {l_2}^3\right)^2\end{gathered} \tag{20}$$

$$[y''(x)]^2 = 144a_4^2[x^4 - 2(l_1 + l_2)x^3 + (l_1 + l_2)^2 x^2], \tag{21}$$

$$\int_0^l EJ(y'')^2\,dx = EJ144a_4^2 \int_0^l [x^4 - 2(l_1 + l_2)x^3 + (l_1 + l_2)^2 x^2]dx, \tag{22}$$

$$\int_0^l EJ(y'')^2\,dx = EJ144a_4^2\left[\frac{l^5}{5} - \frac{2(l_1 + l_2)l^4}{4} + \frac{(l_1 + l_2)^2 l^3}{3}\right], \tag{23}$$

$$\int_0^l (y')^2\,dx = a_4^2\left(2l_1 \cdot {l_2}^2 + {l_2}^3\right)^2 \tag{24}$$

$$\begin{gathered}\int_0^l (y')^2\,dx = a_4^2\left(2l_1 \cdot {l_2}^2 + {l_2}^3\right)^2 + \\ +a_4^2\left\{\frac{16x^7}{7} - \frac{48(l_1 + l_2)l^6}{6} + \frac{36(l_1 + l_2)^2 l^5}{5} + \frac{8\left(2l_1 \cdot {l_2}^2 + {l_2}^3\right)l^4}{4}\right. \\ \left. - \frac{12\left(2l_1 \cdot {l_2}^2 + {l_2}^3\right)(l_1 + l_2)l^3}{3}\right\}\end{gathered} \tag{25}$$

The critical force is determined from the expression [11]:

$$P_{\text{n\_cr}} = \int_0^l EJ(y'')^2\,dx \Big/ \int_0^l (y')^2\,dx. \tag{26}$$

It is equal to:

$$P_{\text{n\_cr}} = \frac{144EJ\left[\frac{l^5}{5} - \frac{2(l_1+l_2)l^4}{4} + \frac{(l_1+l_2)^2 l^3}{3}\right]}{\left(2l_1 \cdot {l_2}^2 + {l_2}^3\right)^2 + \left\{\frac{16l^7}{7} - \frac{48(l_1+l_2)l^6}{6} + \frac{36(l_1+l_2)^2 l^5}{5} + \frac{8\left(2l_1 \cdot {l_2}^2 + {l_2}^3\right)l^4}{4} - \frac{12\left(2l_1 \cdot {l_2}^2 + {l_2}^3\right)(l_1+l_2)l^3}{3}\right\}} \quad (27)$$

where: l_1=2260 mm; l_2=4630 mm, $P_{\text{n\_cr}} = 0{,}06 \cdot EJ\frac{1}{m^2}$. Dimensionless length reduction factor is:

$$\mu = \pi\sqrt{\frac{\left(2l_1 \cdot {l_2}^2 + {l_2}^3\right)^2 + \left\{\frac{16l^7}{7} - \frac{48(l_1+l_2)l^6}{6} + \frac{36(l_1+l_2)^2 l^5}{5} + \frac{8\left(2l_1 \cdot {l_2}^2 + {l_2}^3\right)l^4}{4} - \frac{12\left(2l_1 \cdot {l_2}^2 + {l_2}^3\right)(l_1+l_2)l^3}{3}\right\}}{144 \cdot l^2\left[\frac{l^5}{5} - \frac{2(l_1+l_2)l^4}{4} + \frac{(l_1+l_2)^2 l^3}{3}\right]}}, \quad (28)$$

i.e., $\mu = 1{,}86$. For the aluminium alloy D16T [4], [5], [28], E= 0,75 x 10^5 MP, σ_{pc} = 200 MPa.

Moment of inertia of an unreinforced shell:

$$J_x = J_y = \frac{\pi D^4}{64}(1 - C^4), \quad (29)$$

$$C = \frac{d}{D} = \frac{274}{280} = 0{,}97857. \quad (30)$$

The moment of inertia at a shell thickness of 3 mm is: $J_x = J_y = 2504.264cm^4$, $EJ_x = EJ_y = 1{,}878198 \cdot 10^6 \text{H} \cdot m^2$. The cross-sectional area of the shell F = 0.0026107 m^2.

The smallest radius of gyration of the cross-section of a thin-walled shell [29] is: $i = \sqrt{\frac{J}{F}} = 0.09794m$. Element flexibility:

$$\lambda = \frac{\mu l}{i}. \quad (31)$$

For the entire installation:

$$\lambda = \frac{\mu l}{i} = \frac{1.86 \cdot 6.89}{0.09794} = \frac{12.8154}{0.09794} = 130.85 \quad (32)$$

Body flexibility $\lambda_0 = 60$, $\lambda > \lambda_0$. Euler's approach is applicable [11] for the forebody:

$$\lambda = \frac{\mu l}{i} = \frac{1.86 \cdot 2.26}{0.09794} = \frac{4.2036}{0.09794} = 42.9 \quad (33)$$

$$P_{\text{n\_cr}} = 0{,}06 \cdot 1{,}878198 \cdot 10^6 = 112.692kN, \quad (34)$$

The displacement of the tip of the cone Δ caused by the bending of the elastic axis is determined approximately from the triangle with the hypotenuse dx [11]. The displacement δl of the apex of the fairing cone along the x-axis due to the inclination of the elastic axis is equal to:

$$\delta l = dx - dx\cos\alpha = 2\sin^2(\alpha/2)\,dx, \quad (35)$$

or

$$\delta l = \frac{\alpha^2}{2} = \frac{(y')^2}{2}dx. \quad (36)$$

Summing δl along the length of the rod, we obtain the displacement along the x-axis due to bending:

$$\delta = \frac{1}{2}\int_0^l (y')^2\, dx, \tag{37}$$

$$\alpha = \sqrt{\frac{P_{\text{n\_cr}}}{EJ}} = 0.244949\frac{1}{m}. \tag{38}$$

The curvilinear shape of the cantilever corresponds to $cos\,\alpha \cdot l = 0$ or $\alpha \cdot l_1 = \pi/2$ [30]. When the maximum speed is reached, the total load is equal to $P_{\Sigma}(t) = 536kN$. The critical force for the cantilever part $n = 2$ is

$$P_{\text{n\_cr1}} = \frac{\pi^2 EJ}{n(\mu l_1)^2} = 1503.3kN, \tag{39}$$

and the whole tubular rod:

$$P_{\text{cr max}} = \frac{\pi^2 EJ}{(\mu(l_1 + l_2))^2} = 712kN. \tag{40}$$

The stability condition $P_{\Sigma}(t) < P_{\text{cr max}}$ is satisfied [31]. In this case, the stability margin is $n = 1.33$. The bend of the cantilever bow corresponds to the dependence:

$$y = A\, sin\frac{\pi x}{2l_1}. \tag{41}$$

The displacement Δ along the y-axis can reach limiting values equal to $\Delta = 6{,}7mm$.

4. CONCLUSIONS

Based on the results of the study, using mathematical modelling, the problem of bending the elastic line of a cantilever tubular rod, limited by support No. 3, was solved. The deflection from the forces of external and internal loads of the outer shell of the movable track installation was also considered. The obtained calculations can be useful for strength testing of rocket launchers, as well as other aviation equipment of various types.

REFERENCES

[1] A. A. Skvortsov, N. A. Khripach, D. V. Zaletov and D. E. Pshonkin, Electromigration processes in silicon single crystals involving melt inclusions, *Research Journal of Pharmaceutical, Biological and Chemical Sciences,* vol. **7**, no. 6, pp. 998-1003, 2016.

[2] V. P. Babak and S. I. Kovtun, Calibration thermoelectric heat flux sensor in the diagnostic system of thermal state of electric machines, *Technical Electrodynamics,* vol. **2019**, no. 1, pp. 89-92, 2019.

[3] B. Kovačic, R. Kamnik and A. Bieliatynskyi, The different methods of displacement monitoring at loading tests of bridges or different structures, *MATEC Web of Conferences,* vol. **53**, 01048, 2016.

[4] L. Obolenskaya, E. Moreva, T. Sakulyeva and V. Druzyanova, Traffic forecast based on statistical data for public transport optimization in real time, *International Review of Automatic Control,* vol. **13**, no. 6, pp. 264-272, 2020.

[5] S. G. Gendler, E. B. Gridina, N. A. Egorova, S. A. Kozyrev and B. B. Sogrin, Methodical fundamentals of air consumption calculation for mine working ventilation at the operation of machines and mechanisms with internal combustion engines, *Bezopasnost' Truda v Promyshlennosti,* vol. **2020**, no. 4, pp. 45-51, 2020.

[6] S. A. Astakhov and V. I. Biryukov, Problems of ensuring the acceleration dynamics of aircraft during track test at a speed of 1600 m/s, *INCAS Bulletin*, vol. **12**, Special Issue, pp. 33-42, https://doi.org/10.13111/2066-8201.2020.12.S.3, 2020.

[7] V. G. Kamchatny, *Features of the dynamics of interaction of high-speed objects with a rail*, Nizhny Novgorod, Intelservis, 2000.

[8] O. Skydan, B. Sheludchenko, S. Kukharets, O. Medvedskyi and Y. Yarosh, Analytical study of multifractal invariant attributes of traffic flows, *Eastern-European Journal of Enterprise Technologies,* vol. **3**, no. 3-99, pp. 22-29, 2019.
[9] A. Kadyrov, K. Balabekova, A. Ganyukov and S. Akhmediyev, The constructive solution and calculation of elements of the unified module of the mobile bridge overcrossing, *Transport Problems,* vol. **12**, no. 3, pp. 59-69, 2017.
[10] M. N. Erofeev, V. V. Spiryagin, D. A. Pankin, A. I. Chmykhalo, E. A. Lesyuk and A. V. Chelnokov, Protection against corrosion and restoration of heat exchanger surfaces during repair and operation, *Journal of Machinery Manufacture and Reliability,* vol. **49**, no. 10, pp. 878-883, 2020.
[11] B. V. Zaslavsky, *A short course in strength of materials*, Moscow, Mashinostroyeniye, 1986.
[12] V. G. Aleksandrov, *Aviation materials handbook*, Moscow, Transport Publishing House, 1972.
[13] M. F. Astakhov, A. V. Karavaev, S. Ya. Makarov and Ya. Ya. Suzdaltsev, *Reference book on the calculation of aircraft strength*, Moscow, Oborongiz, 1954.
[14] A. A. Skvortsov, S. M. Zuev and M. V. Koryachko, Contact melting of aluminum-silicon structures under conditions of thermal shock, *Key Engineering Materials,* vol. **771**, 118-123. (2018).
[15] V. Babak, V. Kharchenko and V. Vasylyev, Using generalized stochastic method to evaluate probability of conflict in controlled air traffic, *Aviation,* vol. **11**, no. 2, pp. 31-36, 2007.
[16] J. P. Barnes, Configuration aerodynamics-classical methods applied. Paper presented at the *AIAA AVIATION 2020 FORUM*, vol. **1**, pp. 2020-2708, 2020, doi:10.2514/6.2020-2708
[17] B. K. Khusain, I. A. Shlygina, A. R. Brodsky and M. Z. Zhurinov, Quantum chemical modeling of regents and products in the process of siloxane airgel formation, *Research Journal of Pharmaceutical, Biological and Chemical Sciences,* vol. **7**, no. 5, pp. 3073-3082, 2016.
[18] O. Prentkovskis, A. Beljatynskij, R. Prentkovskiene, I. Dyakov and L. Dabulevičiene, A study of the deflections of metal road guardrail elements, *Transport,* vol. **24**, no. 3, pp. 225-233, 2009.
[19] I. A. Kapitonov and V. I. Voloshin, Strategic directions for increasing the share of renewable energy sources in the structure of energy consumption, *International Journal of Energy Economics and Policy,* vol. **7**, no. 4, pp. 90-98, 2017.
[20] N. A. Bulychev, L. N. Rabinskiy and O. V. Tushavina, Effect of intense mechanical vibration of ultrasonic frequency on thermal unstable low-temperature plasma, *Nanoscience and Technology: An International Journal*, vol. **11**, no. 1, pp. 15-21, 2020.
[21] P. F. Pronina, O. V. Tushavina and E. I. Starovoitov, Study of the radiation situation in Moscow by investigating elastoplastic bodies in a neutron flux taking into account thermal effects, *Periodico Tche Quimica*, vol. **17**, no. 35, pp. 753-764, 2020.
[22] A. A. Orekhov, Yu. A Utkin and P. F. Pronina, Determination of deformation in mesh composite structure under the action of compressive loads, *Periodico Tche Quimica*, vol. **17,** no. 35, 599-608, 2020.
[23] E. L. Kuznetsova and A. V. Makarenko, Mathematic simulation of energy-efficient power supply sources for mechatronic modules of promising mobile objects, *Periodico Tche Quimica*, vol. **15** (Special Issue 1), pp. 330-338, 2018.
[24] A. V. Makarenko and E. L. Kuznetsova, Energy-Efficient Actuator for the Control System of Promising Vehicles, *Russian Engineering Research*, vol. **39**, no. 9, pp.776-779, 2019.
[25] V. A. Zagovorchev and O. V. Tushavina, Selection of temperature and power parameters for multi-modular lunar jet penetrator, *INCAS Bulletin*, vol. **11** (Special Issue), pp. 231-241, 2019, doi:10.13111/2066-8201.2019.11.S.23
[26] V. A. Zagovorchev and O. V. Tushavina, The use of jet penetrators for movement in the lunar soil, *INCAS Bulletin*, vol. **11**, pp. 121-130, 2019, doi:10.13111/2066-8201.2019.11.S.22
[27] S. S. Panda, L. K. Gite, N. Mittal, A. Anandaraj and K. M. Rajan, Parametric aerodynamic evaluation &design of curved brake ring. Paper presented at the *Proceedings – 31st International Symposium on Ballistics, BALLISTICS 2019*, vol. **1**, pp. 816-827, 2019.
[28] L. D. Moreschi and W. Schulz, Aerodynamic resistance in upper atmosphere: Case of the last stage delta rocket fall in argentina, *Computational and Applied Mathematics*, vol. **35**, no. 3, pp. 727-737, 2016.
[29] G. Hertel, *Thin-walled structures*, Moscow, Mashinostroyeniye, 1965.
[30] V. Sundarraj, K. Sundarraj and P. S. Kulkarni, Thermo-fluid analysis of supersonic flow over ballistic shaped bodies with multiple aero-disk spike configurations, *Acta Astronautica*, vol. **180**, pp. 292-304, 2021, doi:10.1016/j.actaastro.2020.12.022
[31] S. Shpund, E. Kelmer, L. Isakov, A. Daher, O. Faibish, D. Heinrich, L. Yosupov, Cornetto project, Paper presented at the *IACAS 2020 – 60th Israel Annual Conference on Aerospace Sciences*, vol. **1**, pp. 648-671, 2020.